❏   317

Wireless power transfer framework for minirobot based on resonant inductive coupling and impedance matching

Kin Yun Lum, Jyi-Shyan Chow, Kah Haur Yiauw
Faculty of Engineering and Technology, Tunku Abdul Rahman University College, Malaysia

Article Info	ABSTRACT
	Minirobots which are under the field of miniature robotics, have a dimension of a few centimetres to even a few millimetres. Conventionally, these small sized robots are usually powered up by batteries. The batteries can take up a lot of space and result in a bulky system. Isolating the energy storage components from the robot itself can provide a good alternative to further down sized the robot. This can be done with the incorporation of wireless power transfer (WPT) technology. However, studies of small-size WPT are usually reported with poor efficiency. The objective of this paper is to present an efficient wireless power transfer framework for the minirobot by employing the resonant inductive coupling together with impedance matching technique. The theory and design process will be discussed. Then, a simple prototyping experiment was conducted to verify the proposed framework. Result showed 35% transfer efficiency had been achieved on a transmission distance of 0.5 cm. The proposed framework had also successfully powered a 4 watts minirobot prototype at about 16% transfer efficiency where its receiver coil was located 3.5 cm above the transmitter coil.

Corresponding Author:

Kin Yun Lum,
Faculty of Engineering and Technology,
Tunku Abdul Rahman University College,
53300 Kuala Lumpur, Malaysia.
Email: lumky@tarc.edu.my

1. INTRODUCTION

In the field of miniature robotics, a minirobot can have a dimension of only a few centimeters, millimeters or even nanometers. These mini sized robots are mainly being utilized to perform tasks in those environments which might be too narrow, too dangerous or too difficult for people to involve and get it done. Other than that, multiple miniature robots can be grouped into swarm robots to carry out microassembly. It is expected that these robots will play an important role in the future when the relevant technologies become mature to support them [1].

The miniaturization of the power source is one of the main bottlenecks for the development of these microscale mobile robots [2]. Existing technology such as battery, does not provide enough energy for these microrobots to operate for a reasonable amount of time [3]. Yet, a battery can easily take up most of its space and result in a bulky system without significantly improving its operation time [4-6]. Furthermore, chemical battery leakage can sometimes be dangerous. In addition, batteries are not eco-friendlier. Lately, scientists and engineers are working very hard to tackle this energy constraint problem. Instead of using battery as power source, they tried to replace it with a system that can harvest energy from the environment [7-8].

What if these robots can be powered up "wirelessly", "battery-less" and efficiently while staying to be safe and eco-friendlier? Wireless power transfer (WPT) makes this possible by supplying power without the need for current-carrying wires or batteries [9-10]. Thus, a microrobot will be able to operate safely for a longer period of time as long as it gets access to the power transmitter. Besides, this technique is very useful in developing waterproof devices, whereby the whole body of the device can be completely sealed up without having the consideration of replacing a dead battery. The wireless power transfer technology can be very beneficial not only to the research and development but also the design within the field of miniature robotics.

Wireless power was initially being invented by Nikola Tesla after 1890 [11]. He conducted a series of public demonstrations based on his wireless power transmission discoveries by applying his knowledge of near-field capacitive and inductive couplings [12]. Unfortunately, Tesla ended up not being able to make his finding a successful commercial product, but his discovery on wireless power had attracted considerable attention around the world. This technology was being brought to the research and development phases in searching for possible safe and efficient applications [13]. Nowadays, wireless power technology simultaneously emanates promising benefits to society, the economy, the environment, not to mention science and technology.

Wireless power transfer (WPT) can be categorized into two which are radiative (long-range transmission) using microwaves and light waves techniques and non-radiative (short range transmission) like magnetic inductive coupling, resonant inductive coupling and capacitive coupling technique [14, 15]. While there are many forms of WPT technologies available, this study will only focus on resonant inductive coupling (associated with impedance matching) due to its better efficiency and longer transmission distance compared to other current non-radiative WPT techniques available as well as safety consideration compared to the radiative WPT techniques.
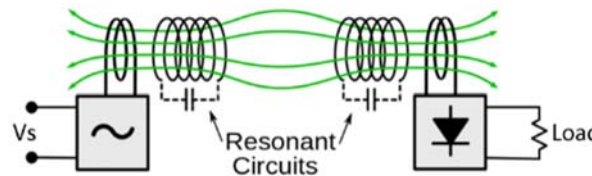

Figure 1. Basic principle representation of resonant inductive coupling technique [16]

Magnetic inductive coupling delivers energy based on the principle of magnetic field induction between two coils, which are the transmitter coil (L_1) and the receiver coil (L_2) [17]. Resonant inductive coupling is the combination of resonator and magnetic inductive coupling as shown by Figure 1. There are two additional resonant circuits, both are tuned at a particular resonant frequency so that energy can be exchanged with greater efficiency at a longer operating distance [18-19]. As a result, it is less susceptible to the variation on coil coupling between L_1 and L_2 as what happened in magnetic inductive coupling system. Consequently, the operation of the resonant inductive coupling is more robust in dealing with the issues of changes in orientation, alignment and distance between L_1 and L_2 in practice [20].

Even though this technique reported higher efficiency, the resonant circuits are generally bulkier, thus prevent its direct implementation on smaller size system. Reduction of the resonant circuits size will degrade its quality factor, hence lead to a lower reported power transfer efficiency [21]. To tackle the above-mentioned problem on a miniature WPT system, impedance matching technique can be incorporated to further enhance the overall transmissible power. This is because impedance matching does allow maximum power transfer for a system with finite source and load impedances. This is analogous to a further tuning of the WPT system to extract as much power as possible from the source [22-23].

This paper presents a WPT framework in powering a minirobot within a vicinity distance of 10 cm. As compared to the conventional inductive coupling WPT system, the resonant inductive coupling associated with impedance matching technique is going to be employed to improve the overall power transfer efficiency. The organization of this paper is as follows. First, the overview of the proposed framework and the system block diagram will be described. Then, the concept of how to implement impedance matching into the proposed WPT framework to enhance the overall power transfer efficiency will be presented. After that, the experimental setup will be discussed. Finally, the obtained results will be verified and discussed.

2.   METHODOLOGY

2.1.   System overview

Figure 2 (a) shows the proposed WPT framework which is used to power a minirobot on top of it. A transmitter circuit will be fit into a casing and then a minirobot will be able to operate when being placed on top of the casing.
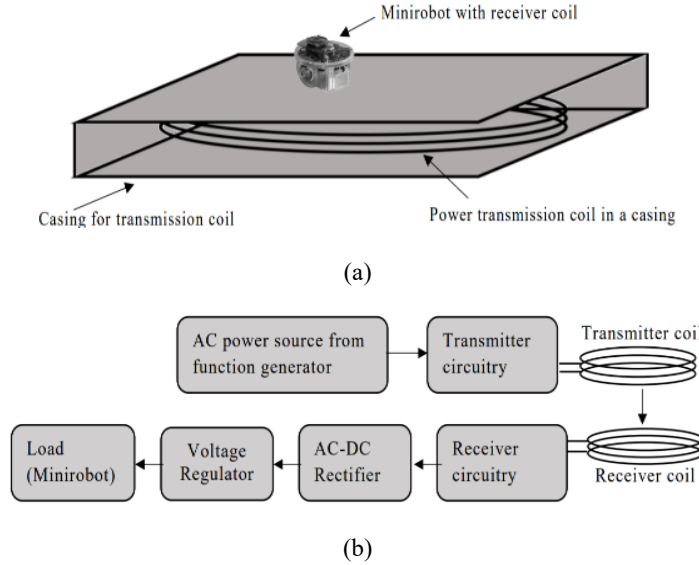

(a)

(b)

Figure 2. (a) Overview of WPT system constructed. (b) Blocks representing parts of the system constructed

The WPT system can be further broken down into a few parts as illustrated in Figure 2 (b). AC power at a particular resonant frequency was used to excite the transmitter coil. Impedance matching circuits were incorporated in the transmitter and receiver circuitries. The resonating magnetic field will provide effective power exchange between the transmitter and receiver. The received power would be converted from AC to DC. It was then regulated to power up the load, which is the minirobot in this case.

2.2.   Concept and theory

Figure 3 is the schematic representation of transmitter circuitry (on the left) and receiver circuitry (on the right). The labels are justified as follow:
- L_1 is the inductance of the transmitter coil while L_2 is the inductance of the receiver coil.
- R_S denoted for the finite source impedance while R_L is the finite load impedance.
- C_1 and C_2 are the compensating capacitors, which are used to tune the coils L_1 and L_2 to operate at the same resonant frequency.
- r_1 and r_2 are the internal power loss of the transmitter and receiver circuit, respectively.
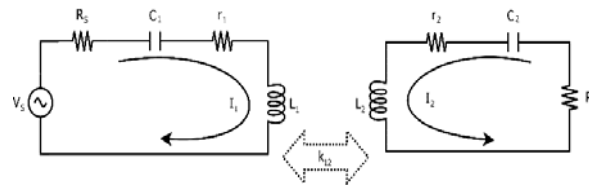

Figure 3. Schematic representation between transmitter and receiver circuitry

Capacitive reactance of transmitter and receiver coil are defined as:

$$X_{C1} = \frac{1}{j\omega C_1} \quad , \quad X_{C2} = \frac{1}{j\omega C_2} \tag{1}$$

and the inductive reactance of transmitter and receiver coil are defined as:

$$X_{L1} = j\omega L_1 \quad , \quad X_{L2} = j\omega L_2 \tag{2}$$

whereby $\omega = 2\pi f$. The mutual inductance exists during the coupling between transmitter and receiver coil, defined as $M_{12} = k_{12}\sqrt{L_1 L_2}$ where k_{12} is the coupling coefficient between the transmitter coil, L_1 and receiver coil, L_2. The mutual reactance can then be expressed as $X_{M_{12}} = j\omega M_{12}$. Next, applying Kirchhoff's Voltage Law:

$$V_s = i_1(R_s + X_{C1} + r_1 + X_{L1}) + i_2 X_{M_{12}} \tag{3}$$

$$0 = i_2(R_L + X_{C2} + r_2 + X_{L2}) + i_1 X_{M_{12}} \tag{4}$$

The transfer efficiency, S_{21} between the transmitter and receiver circuit is expressed as power received at receiver load over maximum transmissible power [16]:

$$S_{21} = \sqrt{\left|\frac{P_{received}}{P_{max\_transmissible}}\right|} = \sqrt{4\left(\frac{i_2}{V_s}\right)^2 R_s R_L} \tag{5}$$

Quality factor of transmitter and receiver coil are defined as:

$$Q_{L_1} = \frac{\omega L_1}{r_1} \quad , \quad Q_{L_2} = \frac{\omega L_2}{r_2} \tag{6}$$

During resonance, $|X_{Cn}| = |X_{Ln}|$ thus,

$$\omega^2 L_1 C_1 = \omega^2 L_2 C_2 = 1 \tag{7}$$

The transfer efficiency, S_{21} in (5) can be determined by solving (3) and (4), and simplification by substituting (6) and (7) to result (8).

$$S_{21} = \frac{2k_{12}\sqrt{Q_{L_1}Q_{L_2}r_1 r_2 R_s R_L}}{k_{12}^2 Q_{L_1}Q_{L_2}r_1 r_2 + (R_S+r_1)(R_L+r_2)} \tag{8}$$

The (8) shows that the transfer efficiency is depending on the coil coupling (k_{12}) quality factor (Q_{L_1}, Q_{L_2}), coil resistive loss (r_1, r_2) and finite source and load impedance (R_S, R_L). Unlike a transformer which employs magnetic core to improve the coil coupling, WPT is unable to do so because the L_1 and L_2 coils are loosely coupled and the magnetizing flux reduces exponentially with the increment of coil separation [24]. There is also no tuning can be done on the quality factor and coil resistive loss because they are fairly constant for a given WPT system. Hence, the adjustment of the source and load impedance provides the room to optimize a particular WPT system. Alike the concept of maximum power transfer, a proper selection of the source impedance, R_S and load impedance, R_L can maximize the power being transferred to the load, thus lead to an improvement in overall transfer efficiency [25, 26].

To determine the optimal R_S and R_L values, taking the derivative of $\frac{dS_{21}}{R_S} = 0$ and $\frac{dS_{21}}{R_L} = 0$ then solving for the R_S and R_L, respectively.

$$R_{S_{opt}} = r_1\sqrt{1 + k_{12}^2 Q_{L_1}Q_{L_2}} \tag{9}$$

$$R_{L_{opt}} = r_2\sqrt{1 + k_{12}^2 Q_{L_1}Q_{L_2}} \tag{10}$$

A typical impedance matching network such as L-match, pi-match, or T-match can be employed here for either impedance up or impedance down transformation to transform the existing impedance values into the optimal value as shown by (9) and (10).

2.3. Experiment setup

2.3.1. Coil construction

All the coils were constructed using enameled copper wire with a thickness of 1.2 mm. The transmitter coil was in flat spiral shape with an outer diameter of 38.5 cm and inner diameter of 1.8 cm. The coil had 18 turns and the gap between each turn is 1 cm. The measured inductance was 69.97 μH with a quality factor, $Q_{L_1} = 94$.

The receiver coil was in cylindrical shape with a diameter of 60 mm. It was a 5 turns coil with a height of 6 mm. Its measured inductance was 2.76 μH and quality factor, $Q_{L_2} = 139$.

2.3.2. Frequency tuning

Both the transmitter coil and receiver coil were compensated with class 1 ceramic capacitor in series to form a resonant LC circuit at a resonant frequency of about 3 MHz. The capacitances of the compensating capacitor was determined by equation $= \frac{1}{2\pi\sqrt{LC}}$.

Since the exact calculated capacitance value was hard to be formed, the nearest capacitance value was chosen instead. Capacitors of 41 pF and 0.92 nF were connected to the transmitter coil and receiver coil respectively. The resonance frequency was once again verified by measuring the reactance value of the LC circuits at different frequencies. The reactance value was at the lowest during resonance.

2.3.3. Applying impedance matching

As discussed in the previous section, proper selection of R_S and R_L values can improve the overall power transfer efficiency of the designed WPT system. Since the VNA ports are having a fixed characteristic impedance of 50 Ω, impedance matching technique was used to transform this characteristic impedance to the optimal source impedance, $R_{S_{opt}}$ and optimal load impedance, $R_{L_{opt}}$. It was done firstly by measuring the mutual inductance between the transmitter and receiver coils. Then, the coupling coefficient, k_{12} between the coils was determined according to the mutual inductance equation mentioned previously. After that, optimal source impedance, $R_{S_{opt}}$ and optimal load impedance, $R_{L_{opt}}$ were computed using (9) and (10).

A pair of L match networks were employed here to transform the 50 Ω characteristic impedances to the desired optimal source and load impedances as shown in Figure 4 (a). L match network 1 was used to transform the 50 Ω source impedance from VNA port 1 to the desired $R_{S_{opt}}$ while L match network 2 was used to transform the 50 Ω load impedance from VNA port 2 to the desired $R_{L_{opt}}$. Nearest inductance and capacitance values were chosen to form these L match networks. The experiment setup discussed in this section was displayed in Figure 4 (b). It was being assumed that the power loss across this L-match network was negligible.
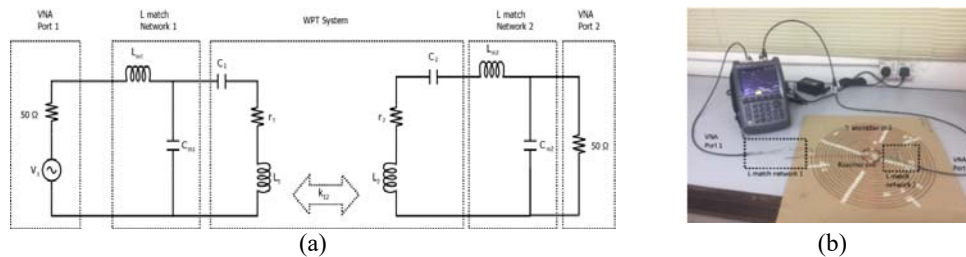

(a)   (b)

Figure 4. (a) Schematic to transform the characteristic impedance of the VNA to the optimal source and load impedance. (b) Experiment setup

2.3.4. Minirobot prototype

The minirobot prototype consisted of one Arduino Nano microcontroller and two 3 V miniature low power DC brush motors. The movement of the minirobot was controlled by individual PWM signals supplied to each of the motor. The received AC power from the receiver circuit was first converted into DC by the bridge rectifier. Then, utilizing the built-in voltage regulator in Arduino Uno, the supply voltage was regulated and used to power up the minirobot prototype. The schematic of the minirobot prototype is displayed in Figure 5.
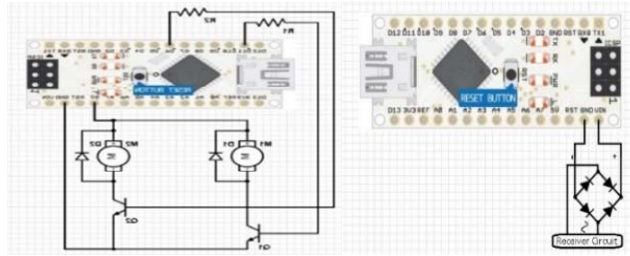
Figure 5. Schematic of minirobot with actuators (on the left) and schematic of minirobot with the power source (on the right)

The dimension of the minirobot prototype was 5 cm in length (L), 7.5 cm in width (W) and 5.5 cm in height (H). Different views of the minirobot prototype were shown in Figure 6. The receiver coil was located 3.5 cm above the ground.
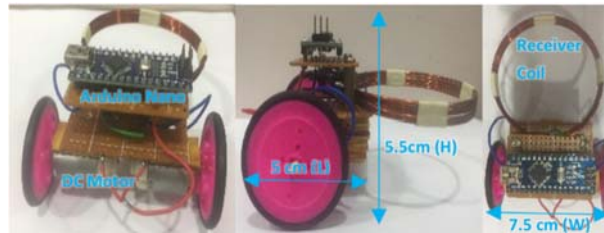

Figure 6. On the left is the front view. At the middle is the side view and on the right is the top view of the minirobot

3.   METHODOLOGY
3.1.   Power requirement of minirobot

First, the power requirement of the minirobot was determined under different working conditions. There were five scenarios simulated to resemble the possible working condition of the minirobot prototype as being stated in following:

- Idle condition: none of the motor was activated
- Normal turning: only one motor was activated at 50% duty cycle.
- Rapid turning: only one motor was activated at 100% duty cycle.
- Normal Forward: Both motors was activated at 50% duty cycle.
- Rapid forward: Both motors were activated at 100% duty cycle.

The consumed power for each respective scenario was measured and tabulated in Table 1. The maximum power required by the minirobot is 4 W.

Table 1. Power consumption of minirobot prototype

Numbers of motor activated	PWM Duty Cycle (%)	Power consumed (W)
0	N/A	0.2
1	50	1
1	100	2
2	50	2
2	100	4

3.2.   Resonant frequency of the coils

The resonant frequency of the constructed coil after compensated with class 1 ceramic capacitors was determined by the coil reactance measurement under frequency sweeping as depicted by Figure 7.

During the resonance, both transmitter and receiver coils exhibited lowest reactance value. However, the resonant frequency of the transmitter coil was at about 3.2 MHz while the receiver coil was at 3.0 MHz. This imperfect frequency tuning was primarily attributed to non-ideal components used. Hence, the operating frequency of this WPT system could only lie between 3.0 – 3.2 MHz and some performance degradation was expected in this design.
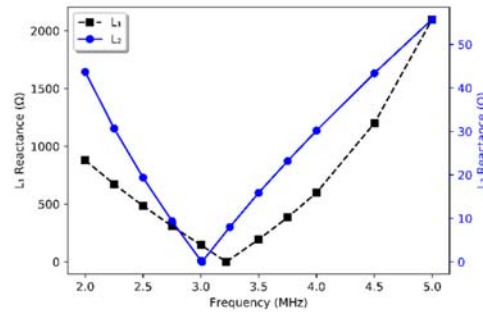

Figure 7. Graph of reactance magnitude against frequency of transmitter coil L_1 and receiver coil L_2

3.3. WPT transfer efficiency

The transfer efficiency of the WPT system was indicated by the S_{21} parameters measured using VNA. Figure 8 (a) shows the transfer efficiency of the proposed design under varying operating frequency at a fixed distance of 0.5 cm. The maximum transfer efficiency obtained at this distance was 35% which occurred at the resonant frequency of 3.09 MHz. This frequency is the middle resonant frequency of the transmitter coil and the receiver coil.

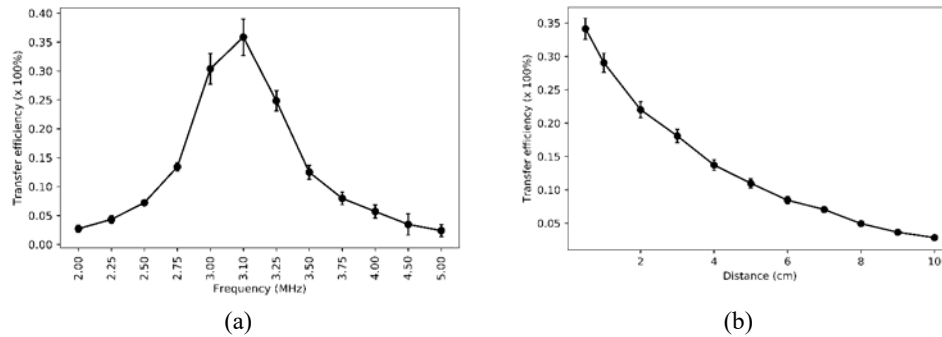
(a)   (b)

Figure 8. (a) Graph of transfer efficiency versus frequency at fixed distance of 0.5 cm. (b) Graph of transfer efficiency versus transmission distance

The transfer efficiency at varying distance up to 10 cm was measured and plotted in Figure 8 (b). The experiment was repeated up to three times to obtain the average and standard deviation. The transfer efficiency dropped accordingly with the distance increment. For example, when the receiver coil is 2.5 cm above the ground, the transfer efficiency is around 20%.

There were larger variations in transfer efficiency measurement when the receiver coil was placed closer to the transmitter coil, which was less than 2 cm. This was because the coil coupling was very sensitive to the coil alignment. Slight tilting in the receiver coil will result in some variation in the coupling coefficient. Besides that, the mutual inductance effect was significant at short distance which could effectively alter the inductance of the transmitter coil and receiver coil. This would result in a displaced resonant frequency and varied the transfer efficiency.

3.4. Power transferred to the minirobot

The designed WPT system was used to power the minirobot. The measured average power received by the minirobot was 4.06 ± 0.02 W. The average sending power was 25.13 ± 1.94 W. The transfer efficiency was around 16% at a transmission distance of 3.5 cm.

Since this study mainly aims to propose a WPT framework for powering a miniaturized system. So, the power loss across the other components, such as rectifier and regulator were all being neglected. The measured transfer efficiency was only dedicated to the WPT system, not the end-to-end efficiency.

4. CONCLUSION

This paper presented an efficient wireless power transfer (WPT) framework for the miniature robots. The novelty of this article lies with the incorporation of the impedance matching circuitry to improve the overall power transmission efficiency of the resonant inductive coupling WPT system for a minirobot. The proposed framework can be served as an alternative powering solution for a minirobot besides batteries or electrical wires due to its reliable transfer efficiency. The involving concepts and theories had been discussed thoroughly. Thereafter, the proposed framework was again verified by experiments. The maximum achievable transfer efficiency of this system was about 35% from the conducted experiment. The transfer efficiency was decreasing gradually with the increment of transmission range. The system also demonstrated a transfer efficiency of about 16% when transferring to a minirobot which has a receiver coil situated 3.5 cm above the transmitter coil.

REFERENCES

[1] Kim D., Hwang K., Park J., Park H. H. and Ahn S., "High-efficiency wireless power and force transfer for a micro-robot using a multiaxis AC/DC magnetic coil," *IEEE Transactions on Magnetics*, vol. 53, no. 6, pp. 1-4, 2017.

[2] Kim D., Hwang K., Park J., Park H. and Ahn S., "Miniaturization of implantable micro-robot propulsion using a wireless power transfer system," *Micromachines*, 8, no. 9, p. 269, 2017.

[3] Sitti M., Ceylan H., Hu W., Giltinan J., Turan M., Yim S. and Diller E. D., "Biomedical applications of untethered mobile milli/microrobots," *Proceedings of the IEEE*, vol. 103, no. 2, pp. 205-224, 2015.

[4] Jiang H., Zhang J., Lan D., Chao K. K., Liou S., Shahnasser H., Fechter R., Hirose S., Harrison M. and Roy S., "A low-frequency versatile wireless power transfer technology for biomedical implants," *IEEE transactions on biomedical circuits and systems*, vol. 7, no. 4, pp. 526-535, 2013.

[5] Ding Z., Zhong C., Ng D. W. K., Peng M., Suraweera H. A., Schober R. and Poor H. V., "Application of smart antenna technologies in simul- taneous wireless information and power transfer," *IEEE Communications Magazine*, vol. 53, no. 4, pp. 86-93, 2015.

[6] Mustapa Zaki, S. Shakir, Y. Yusmarnita and Meor M. S., "Capacitive power transfer in biomedical implantable device: a review," *International Journal of Electrical and Computer Engineering (IJECE)*, vol. 10, no. 2, pp. 935-942, 2019.

[7] Dolev S., Frenkel S., Rosenblit M., Narayanan R. P. and Venkateswarlu K. M., "In-vivo energy harvesting nano robots," *2016 IEEE International Conference on the Science of Electrical Engineering (ICSEE)*, pp. 1-5, 2016.

[8] Han M., *et al.,* "Three-dimensional piezoelectric polymer microsystems for vibrational energy harvesting, robotic interfaces and biomedical implants," *Nature Electronics*, vol. 2, no. 1, p. 26, 2019.

[9] Dai H., Liu Y., Chen G., Wu X., He T., Liu A. X. and Ma H., "Safe charging for wireless power transfer," *IEEE ACM Transactions on Networking (TON)*, vol. 25, no. 6, pp. 3531-3544, 2017.

[10] Lu X., Niyato D., Wang P., Kim D. I. and Han Z., "Wireless charger networking for mobile devices: Fundamentals, standards, and applications," *IEEE Wireless Communications*, vol. 22(2), pp. 126-135, 2015.

[11] Kazuya and Yamaguchi, "The interaction between load circuits and de- cision of frequency for efficient wireless power transfer," *International Journal of Electrical and Computer Engineering (IJECE)*, vol. 8(3), pp. 1331-1335, 2018.

[12] Barman S. D., Reza A. W., Kumar N., Karim M. E. and Munir A. B., "Wireless powering by magnetic resonant coupling: Recent trends in wireless power transfer system and its applications," *Renewable and Sustainable energy reviews*, vol. 51, pp. 1525-1552, 2015.

[13] Kazuya, Yamaguchi, K. Onishi, and Iida K., "Wireless power transfer to a micro implant device from outside of human body," *International Journal of Electrical and Computer Engineering (IJECE)*, vol. 9, no. 3, pp. 1541-1545, 2019.

[14] Mustapa Zaki, S. Shakir, and Yusmarnita Y., "A new design of capacitive power transfer based on hybrid approach for biomedical implantable device," *International Journal of Electrical and Computer Engineering (IJECE)*, vol. 9, no. 4, pp. 2336-2345, 2019.

[15] Dai J. and Ludois D. C., "A survey of wireless power transfer and a critical comparison of inductive and capacitive coupling for small gap applications," *IEEE Transactions on Power Electronics*, vol. 30, no. 11, pp. 6017-6029, 2015.

[16] Wei X., Wang Z. and Dai H., "A critical review of wireless power transfer via strongly coupled magnetic resonances," *Energies*, vol. 7, no. 7, pp. 4316-4341, 2014.

[17] Eteng A. A., Rahim S. K. A., Leow C. Y., Jayaprakasam S. and Chew B. W., "Low-power near-field magnetic wireless energy transfer links: A review of architectures and design approaches," *Renewable and Sustainable Energy Reviews*, vol. 77, pp. 486-505, 2017.

[18] Lu X., Wang P., Niyato D., Kim D. I. and Han Z., "Wireless charging technologies: Fundamentals, standards, and network applications," *IEEE Communications Surveys & Tutorials*, vol. 18, no. 2, pp. 1413-1452, 2016.

[19] Yang C. -W. and Yang C.-L., "Analysis of inductive coupling coils for extending distances of efficient wireless power transmission," *2013 IEEE MTT-S International Microwave Workshop Series on RF and Wireless Technologies for Biomedical and Healthcare Applications (IMWS-BIO)*, pp. 1-3, 2013.

[20] Duong T. P. and Lee J.-W., "Experimental results of high-efficiency resonant coupling wireless power transfer using a variable coupling method," *IEEE Microwave and Wireless Components Letters*, vol. 21, no. 8, pp. 442-444, 2011.

[21] Waters B. H., Mahoney B. J., Lee G. and Smith J. R., "Optimal coil size ratios for wireless power transfer applications," *IEEE Proceedings of International Symposium on Circuits and Systems*, pp. 2045-2048, 2014

[22] Zhong W. and Hui S., "Maximum energy efficiency tracking for wireless power transfer systems," *IEEE Transactions on Power Electronics*, vol. 30, no. 7, pp. 4025-4034, 2015.

[23] Fu M., Yin H., Zhu X. and Ma C., "Analysis and tracking of optimal load in wireless power transfer systems," *IEEE Transactions on Power Electronics*, vol. 30, no. 7, pp. 3952-3963, 2015.

[24] Zhang W. and Mi C. C., "Compensation topologies of high-power wireless power transfer systems," *IEEE Transactions on Vehicular Technology*, vol. 65, no. 6, pp. 4768-4778, 2015.

[25] Kazuya, Yamaguchi, T. Hirata and I. Hodaka, "A general method to parameter optimization for highly efficient wireless power transfer," *International Journal of Electrical and Computer Engineering (IJECE)*, vol. 6, no. 6, pp. 3217-3221, 2016.

[26] Agbinya J. I., "Wireless power transfer," *River Publishers*, vol. 45, 2015.

BIOGRAPHIES OF AUTHORS

Kin Yun Lum was born in Malaysia in 1989. He received the B.S. degree in Microelectronics Engineering and Ph.D degree in Biomedical Engineering from Universiti Teknologi Malaysia, Malaysia in 2012 and 2016 respectively. His current research interests include wireless power transfer system, power electronics and robotic systems.

Jyi-Shyan Chow was born in Malaysia in 1994. He received his degree of Bachelor of Engineering (Honours) Mechatronics from Tunku Abdul Rahman University College in 2018. Currently he is working in an M&E company named PT Power M&E Sdn Bhd. His research interests include wireless power transfer, power transmission and distribution system.

Kah Haur Yiauw was born in Malaysia in 1975. He received the B.E and Ph.D. degrees from University of Wales, Swansea, UK in 1998 and 2005 respectively. He joined Tunku Abdul Rahman University College, Luala Lumpur, Malaysia since 2006, where he is currently a Principal Lecturer. His main areas of research interest are reactive harmonic filters, smart energy management systems and their control systems.